

PASSIVATING MC-SI SOLAR CELLS USING $\text{SiN}_x\text{:H}$: FROM MAGIC TO PHYSICS

I. G. Romijn, W. J. Soppe, H. C. Rieffe, A. R. Burgers, A. W. Weeber
ECN Solar Energy, P. O. Box 1, 1755 ZG Petten, The Netherlands
email: weeber@ecn.nl

ABSTRACT: Bulk passivation with $\text{SiN}_x\text{:H}$ has been so far a barely understood effect that can only be optimized for cell production in an empirical way. In this study we determine the structural properties of $\text{SiN}_x\text{:H}$ layers and relate these to both the deposition parameters and its passivating qualities for solar cells. These structural properties, such as Si-N and Si-H bond densities, of the $\text{SiN}_x\text{:H}$ layers deposited with either N_2 , NH_3 or ND_3 and silane are measured with FTIR. We show that Si-N bond density is an important parameter governing both the bulk and surface passivation of the $\text{SiN}_x\text{:H}$ layers. We find optimum bulk and surface passivation for Si-N bond densities of $1.3 \cdot 10^{23} \text{ cm}^{-3}$, regardless of nitrogen containing precursor gases used and regardless of the wafer quality. This study indicates that FTIR analysis gives us a quick and reliable tool to check the quality and properties of $\text{SiN}_x\text{:H}$ layers. This will allow optimization of $\text{SiN}_x\text{:H}$ deposition systems without having to make complete solar cells.

Keywords: Antireflection coating, Silicon-Nitride, Passivation.

1 INTRODUCTION

Hydrogenated amorphous silicon nitride layers (a- $\text{SiN}_x\text{:H}$) layers have become a very important part of modern silicon PV technology. They act as an anti-reflection coating, and provide bulk and surface passivation, important means for optimizing mc-Si solar cells and reaching high efficiencies [1].

Passivating $\text{SiN}_x\text{:H}$ layers can be deposited using Plasma Enhanced Chemical Vapor Deposition (PECVD) techniques using nitrogen and silicon containing precursor gasses. One of the key issues of our research is to combine excellent bulk and surface passivation on low cost silicon with easy to handle gasses. Relations between structural properties and the bulk and surface passivating qualities need to be known for better understanding of the physics behind passivation by $\text{SiN}_x\text{:H}$. So far, passivation with $\text{SiN}_x\text{:H}$ has been an phenomenon that can only be optimized for cell production in an empirical way. This study provides means to determine passivating qualities of $\text{SiN}_x\text{:H}$ independently of the deposition method, and without making solar cells. Therefore, process optimization and problem solving in production can be done separately from the rest of the cell processing with simple Fourier Transform Infrared (FTIR) analysis, leading to much quicker results, and thus saving time and effort.

Mäckel and Ludemann studied the properties of $\text{SiN}_x\text{:H}$ layers made with NH_3 and SiH_4 , but focused on the structural properties and surface passivation [2]. Hong et al [3] showed that higher densities of $\text{SiN}_x\text{:H}$ layers improves the bulk passivation properties. At the 19th EPVSEC ECN presented for the first time ever, relations between structural properties and both surface and bulk passivation of $\text{SiN}_x\text{:H}$ deposited using N_2 [4]. Si-N bond density of the $\text{SiN}_x\text{:H}$ layers is the important parameter that determines the diffusivity of H in the layer and, thus, the passivating properties. An optimal Si-N bond density was found for bulk passivation. Since the Si-N bond density is related to the mass density [5] our hypothesis is that layers with lower Si-N bond densities are too open and H_2 is formed in the layer that will effuse into the ambient. On the other hand in layers with higher Si-N bond densities, too dense layers, the H-diffusivity is too low for a good bulk passivation during short firing anneals.

This first study is now extended to the use of NH_3 and deuterated ammonia (ND_3). The use of ND_3 sheds

more light on the role of hydrogen in the $\text{SiN}_x\text{:H}$ layer and its deposition mechanisms. The $\text{SiN}_x\text{:H}$ layers are deposited on mc-Si wafers of different quality, using various deposition parameters.

2 EXPERIMENT

2.1 Approach

The physics behind the passivating properties of $\text{SiN}_x\text{:H}$ layers is investigated in three steps:

- Deposition of layers on double polished Cz-Si wafers for FTIR analysis to obtain bond densities and relating those to the deposition parameters;
- Application of the examined layers on solar cells; determination of bulk passivating quality by measuring V_{oc} and $\text{IQE}_{(100\text{nm})}$, and relating these to the structural properties.
- Application of the examined layers on FZ Si wafers; determination of surface passivation by measuring τ_{eff} , and relating these to the structural properties;

2.2 Deposition of $\text{SiN}_x\text{:H}$ layers

We deposited $\text{SiN}_x\text{:H}$ layers with three different types of nitrogen-containing precursor gases; nitrogen (N_2), ammonia (NH_3) and deuterated ammonia (ND_3). This will allow us to determine whether fundamental relations exist independent of the process gases. Silane (SiH_4) was used as silicon precursor gas. The $\text{SiN}_x\text{:H}$ layers were deposited using the in-line microwave remote PECVD system at ECN at different process parameters such as pressure and gas flows.

2.3 FTIR analysis

We determined the bond densities within the nitride layers using FTIR spectroscopy. From the transmission spectrum of the $\text{SiN}_x\text{:H}$ layers deposited on Si substrates the absorption spectrum (k) of the single layer of $\text{SiN}_x\text{:H}$ was calculated according to the method reported by Maley (see figure 1 and 2) [6]. Subsequently, the bond densities are calculated by integrating the different absorption peaks and multiplying with a proportionality constant [7,8]. This more detailed analysis allowed us to improve the accuracy compared to previously published data [4,9]. The absolute values for different bond densities are slightly shifted when compared to our previous publications [4,9], but their behavior relative to deposition parameters remains the same.

In hydrogenated silicon nitride layers, usually three

different bonds are investigated: the Si-N, Si-H and N-H bond density. The use of ND₃ will in principle give us two more bonds: Si-D and N-D [10]. Since the position of the absorption peaks depends on the vibration energy, we expect the Si-D and N-D peaks to shift down by a factor of $\sqrt{2}$ with respect to the Si-H and N-H, due to the larger mass of the deuterium. The N-D peak (expected at ~ 2362 cm⁻¹; N-H ~ 3340 cm⁻¹) can be seen in figure 2. Unfortunately, the Si-D peak, expected at ~ 1530 cm⁻¹, was not discernable from the phonons in the substrate.

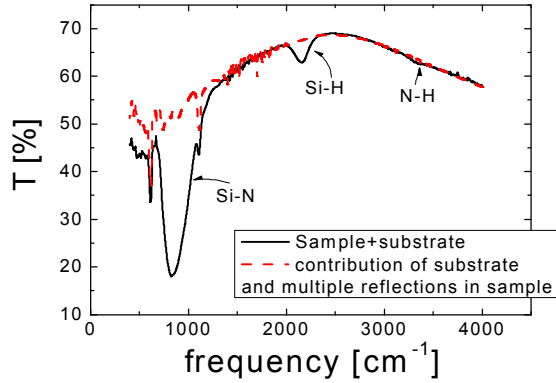


figure 1: Typical transmission spectrum. Absorption (k) is calculated from the difference of the total transmission (solid line) and the calculated contributions of the substrate and multiple reflections in the sample (dashed line).

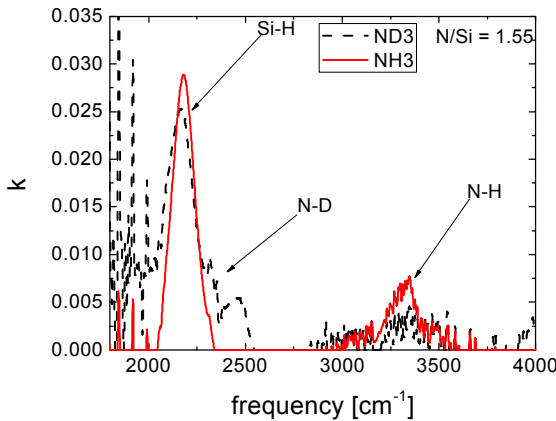


figure 2: Absorption peaks (k) calculated from the difference of the total transmission for layers deposited with NH₃ and ND₃ (same deposition parameters). The N-D peak appears while the Si-H and N-H peak reduce in height for the ND₃ spectrum.

3. EXPERIMENTAL RESULTS AND DISCUSSION

3.1 SiN_x:H structure for different process parameters

In figure 3 and 4 the Si-N bond density for three nitrides deposited with NH₃, ND₃ and N₂ as precursor gasses are shown as a function of the N/Si containing gas flow ratio, and for different deposition pressures. For all nitrides the Si-N bond densities increase for increasing N/Si flow ratio, and are higher for lower deposition pressures. The refraction index n increases with decreasing Si-N bond density and decreasing N/Si flow ratio, which is shown qualitatively by the arrow in the graphs. The absolute values for the nitrides deposited

with N₂ or NH₃ are similar for similar flow ratios. However, the nitrides deposited with NH₃ (and ND₃) are stronger dependent on the flow ratio than the nitrides deposited with N₂, especially at lower pressures ($p = 0.2$ mbar). The deuterated SiN_x layers show the same increasing behavior as layers deposited with NH₃, but are lower in absolute value when deposited at the same pressure (see figure 3).

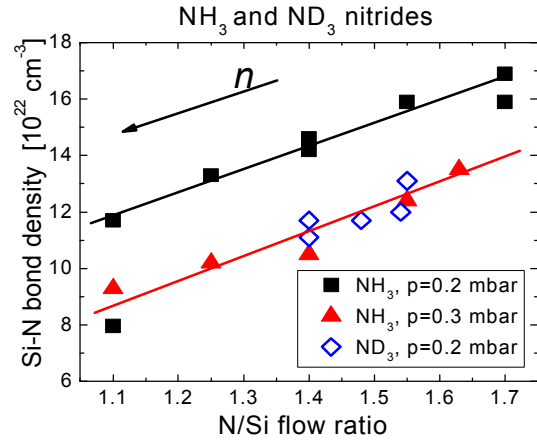


figure 3: Si-N bond density versus the N/Si flow for nitrides deposited with NH₃ and ND₃ at different pressures. Errors are roughly the symbol size.

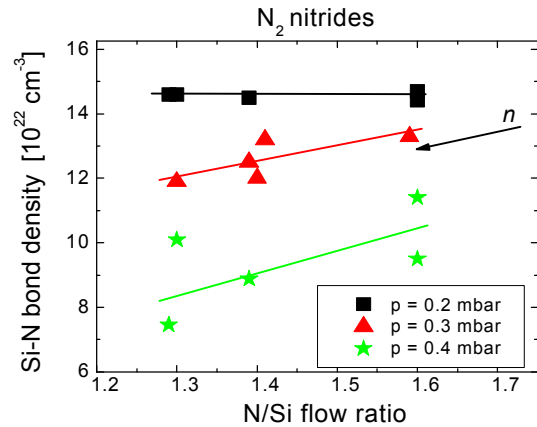


figure 4: N-Si bond density vs N/Si flow ratio for nitrides deposited with N₂ at different pressures. Errors are roughly the symbol size.

The increase in Si-N bond density with increasing N/Si flow ratio is easily understood. Elastic Recoil Detection (ERD) measurement on our layers show that the N/Si atomic ratio in our layers increases linearly with the N/Si flow ratio for the regime measured [11], a higher N/Si atomic ratio will allow more Si-N bonds to be formed. This corresponds to the results of Mäckel and Ludemann [2], who already showed that the Si-N bond density increases with increasing N/Si atomic ratio in the layer. While their layers were deposited with a direct plasma the values reached are comparable to our remote plasma SiN_x:H layers.

The increase of Si-N bond density for decreasing pressures is due to properties of our remote MW PECVD. In our system, the nitrogen containing gas is fed in near the plasma source, while the silane gas is fed in just above the samples. Higher pressures will confine the plasma closer to the plasma source, and less reactive N-

containing species will reach the substrate. This will cause the formation of more Si-rich $\text{SiN}_x\text{:H}$ layers that are known to be less dense. A more detailed description of the plasma chemistry can be found in other publications [12,13]. The difference in pressure and N/Si flow ratio dependence between the nitrides deposited with N_2 and NH_3 , is caused by the difference in ionization energy for N-N (9.81 eV) and H-NH₂ (4.65 eV) [14]. More detailed investigations, using optical emission spectroscopy to detect the different radicals in the plasma, are needed to give a final answer.

The lower Si-N bond density of the deuterated nitride, when compared to the nitride deposited with NH_3 , is due to the difference in dissociation rate of NH_3 and ND_3 . This dissociation rate depends on the vibration frequency of the N-D or N-H in the molecule, which is lower for N-D.

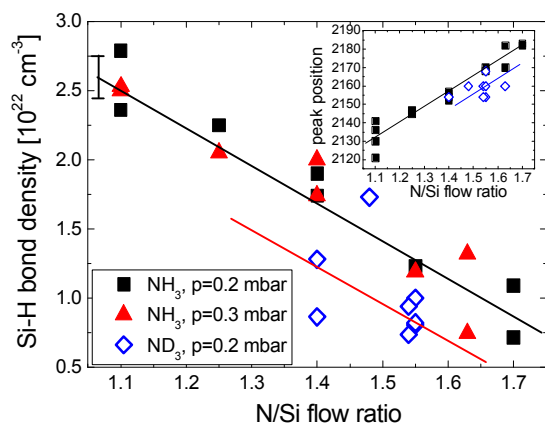


figure 5: Si-H bond density and the Si-H peak position (inset) versus the N/Si flow ratio for the NH_3 and ND_3 nitrides. An indication of the error is given at the left side of the graph.

We observed that for our layers the majority (>90%) of H is bonded to Si. Therefore, besides the Si-N bond density, we focus on the Si-H bond density. In figure 5 the Si-H bond density is shown for the NH_3 and ND_3 nitrides. The insert shows the Si-H peak position as a function of the N/Si flow ratio. For both nitrides, the Si-H bond density decreases with increasing N/Si ratio. At the same time, the Si-H peak position shifts to higher wavenumbers, indicating a change to more N- instead of Si-back-bonding, which is expected at higher N/Si flow ratios. Higher N/Si flow ratios will favor the formation of Si-N over that of Si-H. The N-H bond density will increase as well, but remains small compared to the Si-H bond density. Therefore, at higher Si-N bond densities, the total hydrogen content of the layer decreases.

Surprisingly, contrary to the Si-N bond density, there is no pressure dependence found for the Si-H bond density. This seems unlikely, and could be hidden in the error margin of the Si-H bond densities.

Although the nitrides deposited with NH_3 and ND_3 display the same behavior, the differences are also clear: The Si-H bond density in the layers deposited with ND_3 is 75% of that in the corresponding layer deposited with NH_3 . This means that about 25% of the hydrogen in the $\text{SiN}_x\text{:H}$ layers stems from ammonia, while 75% stems from silane. The peak position is also lower for the layers deposited with ND_3 , revealing a shift to more Si- than N-back-bonding of the Si-H bonds. This is in agreement with the lower Si-N bond densities for the ND_3 nitrides

when compared to the NH_3 nitrides.

3.2 Bulk and surface passivation as a function of Si-N bond density

It was previously shown by us that the Si-N bond density ($[\text{Si-N}]$) is the key parameter for bulk passivation [4,9]. Figure 6 shows the V_{oc} of cells made with $\text{SiN}_x\text{:H}$ layers deposited with N_2 or NH_3 . Wafers of less quality (A) and wafers of better quality (B) were used. From figure 6 it can be seen that:

- The V_{oc} for cells with $\text{SiN}_x\text{:H}$ layers deposited with N_2 or NH_3 have the same dependence of the Si-N bond density.
- The maximum V_{oc} for both material qualities is found at the same Si-N bond density, viz. $1.3 \cdot 10^{23} \text{ cm}^{-3}$. The difference is that for the better quality higher V_{oc} values are found for a broader range of Si-N bond densities.

We were not able to make solar cells with $[\text{Si-N}] < 9 \cdot 10^{22} \text{ cm}^{-3}$ or $[\text{Si-N}] > 1.5 \cdot 10^{23} \text{ cm}^{-3}$, because these layers became too inhomogeneous at larger areas.

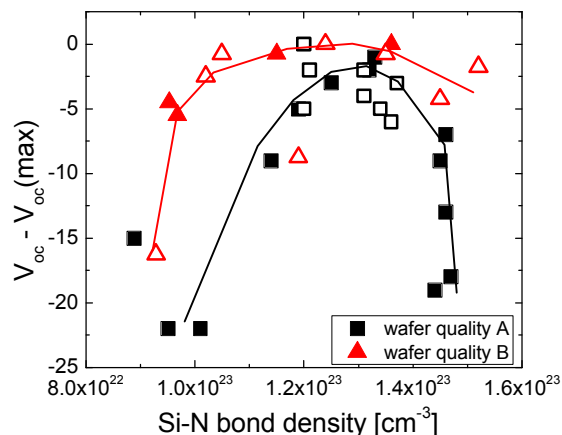


figure 6: $V_{oc} - V_{oc(max)}$ of mc-Si solar cells versus the Si-N bond density. The squares show the V_{oc} for cells made of average quality (A), the triangles show V_{oc} for cells made of good wafer quality (B). Closed symbols: N_2 nitrides; open symbols: NH_3 nitrides. The lines are guides to the eye.

V_{oc} is determined by both the bulk and surface passivation. To investigate the dependence of the Si-N bond density on bulk passivation the IQE at 1000 nm is shown in figure 7. When the wafer quality is less (squares in graph), the V_{oc} follows the IQE at 1000 nm indicating V_{oc} is mainly influenced by the bulk properties of the solar cell. In the case of better wafer quality (triangles) however, the IQE remains constant down to very low Si-N bond densities ($1 \cdot 10^{23} \text{ cm}^{-3}$). In this case, the bulk properties remain constant and smaller changes in V_{oc} (<5 mV) are caused by differences in surface passivation. At the lowest bond densities, the bulk passivation is drastically reduced, resulting in an additional loss in V_{oc} of about 10 mV.

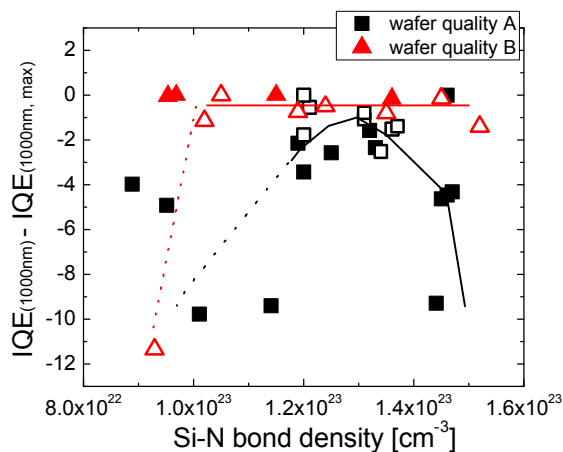


figure 7: IQE at 1000 nm for the different solar cells. Again the difference between the different wafer quality is clearly visible. Closed symbols: N_2 nitrides; open symbols: NH_3 nitrides. The lines are guides to the eye.

The effective lifetime of charge carriers in FZ wafers coated with $SiN_x:H$ layers is a good measure of the surface passivation. In figure 8 we show the effective lifetimes for N_2 -grown nitrides with the different Si-N bond densities, before and after a very long anneal (60 min at 800 °C).

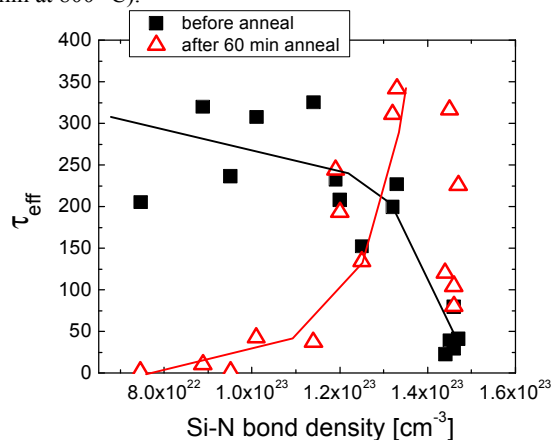


figure 8: effective lifetimes of charge carriers in FZ wafers with $SiN_x:H$ layers before and after anneal (60 mins, 800 °C). The lines are guides to the eye.

The figure shows that good initial surface passivation (large τ_{eff}) can be obtained for layers with low Si-N bond densities, but that this surface passivation is not thermally stable after a 60 minute anneal (although the much shorter firing of solar cells does not influence the τ_{eff} this much [12]). At high Si-N bond densities, the initial τ_{eff} is low, but after a long anneal the values improve drastically. Around $[Si-N] \sim 1.3 \cdot 10^{23} \text{ cm}^{-3}$, the layers do not change and τ_{eff} remains constant at high values. At these bond densities, V_{oc} for wafers of good quality reaches its maximum (see figure 6, wafer quality B) which we contribute to the good and stable surface passivation. At higher Si-N bond densities there is a large variation in lifetime after annealing. This means that the best and most stable processing is found at a Si-N bond density of $1.3 \cdot 10^{23} \text{ cm}^{-3}$, the same density as for the best bulk passivation.

Combining the results for the bulk and surface passivation, we find optimum values for Si-N bond

densities of $1.3 \cdot 10^{23} \text{ cm}^{-3}$ for both, regardless of the type of $SiN_x:H$ used and regardless of the wafer quality.

4. CONCLUSIONS

We have shown that for $SiN_x:H$ layers deposited with our MW PECVD system the N/Si flow ratio and the deposition pressure are important processing parameters. The Si-N and Si-H bond densities of layers deposited with N_2 , NH_3 or ND_3 show very similar relations to the N/Si flow ratio and the pressure p . Comparing the Si-N and Si-H bond densities found for NH_3 and ND_3 grown layers, we find that only 25% of the hydrogen in the $SiN_x:H$ layers stems from the ammonia precursor gas, while 75% stems from the silane.

The Si-N bond density found via the FTIR analysis is an important parameter for the solar cell characteristics, governing both the bulk and surface passivation of the $SiN_x:H$ layers. We find optimum bulk and surface passivation for Si-N bond densities of $1.3 \cdot 10^{23} \text{ cm}^{-3}$, regardless of the type of $SiN_x:H$ used and regardless of the starting wafer quality. Cells made from good quality wafers however, show a much broader maximum in V_{oc} versus the Si-N bond densities, allowing a larger variation in processing parameters. The almost constant IQE at 1000 nm confirms this.

This study indicates that FTIR analysis of the $SiN_x:H$ layers gives us a quick and reliable tool to check the quality and properties of different $SiN_x:H$ layers. This will allow optimization of $SiN_x:H$ deposition systems without having to make complete solar cells.

6 ACKNOWLEDGEMENTS

This work was financially supported by NovemSenter in the DEN program.

7 REFERENCES

- [1] S. Winderbaum, F. Yun, O. Reinhold, J. Vac. Sci. Techn. A 15, 1020 (1997).
- [2] H. Mäckel and R. Lüdemann, J. Appl. Phys. 92, 2602 (2002).
- [3] J. Hong, et al., J. Vac. Sci. Techn. B: 21, 2123 (2003)
- [4] A. Weeber, et al., Proc. 19th EPVSEC 2004 Paris p1005.
- [5] A.J.M. van Erven, Master Thesis, Eindhoven University of Technology.
- [6] N. Maley, Phys. Rev. B 46, 2078 (1992).
- [7] F. Giorgis et al, Phil. Mag. B 46, 2078 (1992).
- [8] E. Bustarret et al, Phys. Rev. B 38, 8171.
- [9] A. W. Weeber, et al., Proc. 31st IEEE PV Specialists Conf. 2005 Orlando.
- [10] C. Boehme and G. Lucovski, Mat. Res. Soc. Symp. Proc. 609 A26.7.1 (2000)
- [11] I. Romijn et al., to be published
- [12] W. Soppe et al., Progress in Photovoltaics, 13, 1 (2005)
- [13] W. Soppe et al., to be published.
- [14] Rieffe et al., Proc. 17th EPVSEC 2002, Rome